© 2026 IEEE. Personal use of this material is permitted. Permission from IEEE must be obtained for all other uses, in any current or future media, including reprinting/republishing this material for advertising or promotional purposes, creating new collective works, for resale or redistribution to servers or lists, or reuse of any copyrighted component of this work in other works.
This is the author's accepted manuscript. The final version is published in IEEE Transactions on Visualization and Computer Graphics, vol. 32, no. 5, pp. 4041-4050, 2026. DOI: 10.1109/TVCG.2026.3679127

ChillFactor: A Highly-Responsive Non-Contact Cooling Feedback Interface for VR Headsets Based on Alcohol Mist Evaporation

Jiayi Xu, Chia-An Fan, Yuan Guo, Yoshihiro Kuroda, and Masahiko Inami

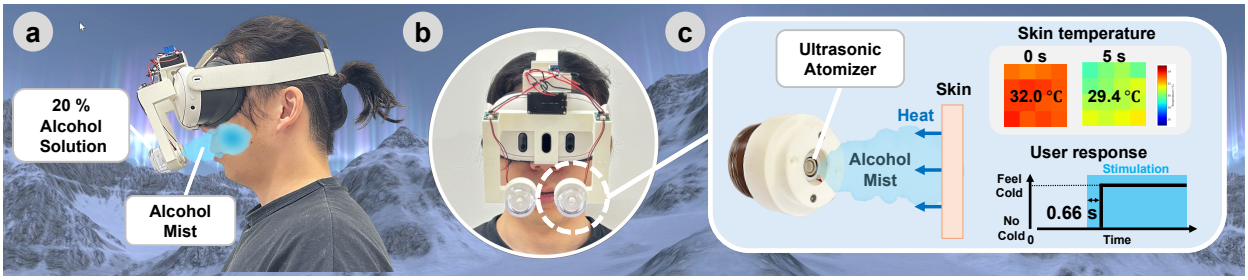


Fig. 1: Overview of the ChillFactor System: A highly responsive, non-contact cooling feedback interface for VR headsets. The system ultrasonically atomizes a 20 % alcohol solution to generate a mist around the skin, providing immediate cold sensation through evaporation. The figure shows (a) the VR scene viewed through the HMD, (b) the integrated system worn by the user, and (c) the cooling module with an ultrasonic atomizer used to generate the alcohol mist. The cooling module can induce a skin temperature drop of 2.6 ℃ within 5 seconds, and users reported perceiving the cooling effect only 0.66 seconds after the stimulation onset.

Abstract—Cooling feedback has been shown to improve user experience in virtual reality. However, many existing methods face limitations, such as requiring skin contact, relying on airflow, having bulky components, or delivering unstable sensations. These issues limit their applicability to wearable systems, especially in scenarios demanding high responsiveness and perceptual consistency. We propose ChillFactor, a highly responsive, non-contact cooling interface for head-mounted displays (HMDs). It uses ultrasonic atomization of a predetermined alcohol solution to generate evaporative cooling near the skin, reducing airflow-induced artifacts and providing relatively consistent cold sensations. To validate the design, we first evaluated the system's cooling performance. At maximum output, it lowered skin temperature by approximately 2.6 ℃ within five seconds, a rate sufficient to induce an almost immediate perception of cold. We subsequently integrated ChillFactor into an HMD and conducted a user study with 12 participants in immersive VR scenarios. Participants reported perceiving the cold within 0.66 seconds and noted significantly higher levels of presence and realism compared to conditions without cooling feedback, demonstrating the system's effectiveness in enhancing immersion through rapid and adjustable thermal cues. This work provides a practical foundation for non-contact cooling feedback and expands the design space for multisensory interaction in virtual environments.

Index Terms—Thermal feedback, cold sensation, non-contact haptic interface, virtual reality.

1 Introduction

With the continuous advancement of multisensory interaction technologies, thermal feedback has emerged as a critical modality for improving the perceived immersion and realism in virtual reality (VR) environments. Among various thermal cues, cold sensations are particularly significant, as they contribute to the simulation of environmental factors (e.g., wind, snow), material properties (e.g., metal, ice), physiological reactions (e.g., shivering, goosebumps), and emotional states such as discomfort, anxiety, or fear [1, 12]. These cold-based cues help create richer, more believable virtual experiences that engage users on a deeper perceptual level.

Various cooling feedback methods have been explored, including conductive [3,5,6,10,11,15,20–22,29], convective [4,7,14,19,26–28], radiative [13], chemosensory [2], and evaporative approaches [9,16–18]. Among them, evaporative cooling has received attention as a promising non-contact strategy, as it enables rapid cooling without direct skin contact or the need for a pre-cooled medium. One approach uses focused ultrasound to accelerate the evaporation of water mist near the skin [16–18], offering fast and localized cooling but relying on bulky phased-array transducers that limit wearability. Another method uses alcohol-soaked cotton with a fan to promote evaporation [9], which is power-efficient and wearable but cannot maintain alcohol concentration over time, leading to unstable cooling intensity. This inconsistency presents challenges for VR scenarios that require continuous and reliable feedback.

To address these limitations, we propose ChillFactor, a non-contact cooling feedback interface designed for integration into head-mounted displays (HMDs), as shown in Fig. 1. The system generates a fine mist by ultrasonically atomizing an alcohol solution with a predefined concentration, producing evaporative cooling near the skin without requiring skin contact or airflow stimulation. Unlike airflow-driven systems where the alcohol concentration gradually decreases, ChillFactor maintains a relatively steady concentration, helping to provide more consistent thermal feedback for VR content. This steady feedback promotes crossmodal congruency [25], narrowing the perceptual gap between virtual and physical environments through consistent multisensory integration. Furthermore, its compact structure and high temporal responsiveness make it particularly suitable for multimodal interactions synchronized with dynamic virtual experiences.

The main contributions of this work are as follows:

- We propose ChillFactor, a novel non-contact cooling interface based on evaporative cooling, which produces a mist near the skin by ultrasonically atomizing an alcohol solution with a predefined concentration, enabling immediate perception of cold through

- *Jiayi Xu, Chia-An Fan, and Masahiko Inami are with The University of Tokyo. E-mail: xu.jiayi@star.rcast.u-tokyo.ac.jp.*
- *Yuan Guo is with City University of Hong Kong.*
- *Yoshihiro Kuroda is with University of Tsukuba.*

Manuscript received xx xxx. 201x; accepted xx xxx. 201x. Date of Publication xx xxx. 201x; date of current version xx xxx. 201x. For information on obtaining reprints of this article, please send e-mail to: reprints@ieee.org. Digital Object Identifier: xx.xxxx/TVCG.201x.xxxxxxx

evaporation.

- We conducted user studies to evaluate the effects of cue distance and mist intensity on cold sensation, providing empirical evidence for parameter optimization in non-contact cooling feedback systems.
- We integrated the cooling interface into a VR headset, enabling thermal feedback to be synchronized with virtual events, and validated its effectiveness in enhancing perceived immersion, involvement, and thermal realism based on subjective user evaluations.

2 Related Work

In this section, we first review prior work on cooling feedback interfaces, categorized by their underlying heat transfer mechanisms: conduction, convection, radiation, chemosensory stimulation, and evaporation. Based on this review, we then position our work within the context of evaporative cooling approaches.

2.1 Conductive Cooling-Based Methods

Conductive cooling typically employs thermoelectric modules, such as Peltier elements [5, 6, 11, 15, 20, 22, 29], which regulate the temperature of a contact surface through electrical current, thereby reducing the temperature of the skin in contact. While this approach provides effective and controllable cooling, it often requires additional heat dissipation structures to maintain efficiency, resulting in increased system complexity and power consumption. Other implementations utilize modules filled with chilled air or water, or directly employ liquid water as a heat transfer medium. Although these methods can offer strong cooling performance [3, 10, 13, 21], their reliance on continuous skin contact can complicate integration with other haptic modalities, such as vibration or pressure feedback, particularly in space-constrained wearable systems.

2.2 Convective Cooling-Based Methods

Convective cooling operates by accelerating airflow to remove heat from the skin. Airflow-based implementations are the most common [4, 7, 14, 19], widely adopted in both academic prototypes and commercial VR products for their simplicity and low cost. However, the cooling intensity of ambient airflow is inherently limited. Xu et al. [26–28] proposed a system that utilizes vortex tubes to cool compressed air to near 0 °C, delivering stronger cooling stimuli. While effective in terms of cooling power, such systems require bulky compressors and have limited applicability in wearable contexts.

2.3 Radiative Cooling-Based Methods

Radiative cooling leverages the exchange of infrared radiation between a low-temperature surface and the skin. Kume et al. [13] introduced a non-contact approach using cryogenically cooled insulating materials to deliver cold sensations via thermal radiation. This method offers a high degree of perceptual purity and avoids physical contact or airflow. However, to maintain effectiveness, the user must be isolated from surrounding heat sources, and the system requires large cooling components, limiting its suitability for integration into head-mounted or wearable VR devices.

2.4 Chemosensory Stimulation-Based Methods

Chemosensory stimulation induces cold sensations by activating cold receptors (e.g., TRPM8) without actual temperature reduction. ChemicalTrigger, proposed by Lopes et al. [2], uses aerosols containing menthol and capsaicin to stimulate thermal receptors in the nasal mucosa. While capable of reliably eliciting thermal sensations, this approach depends on stimulation of sensitive mucosal tissue, and the dispersion of aerosols can lead to inconsistent timing and strength of perception. Additionally, the accompanying olfactory stimuli may interfere with the immersive experience.

2.5 Evaporative Cooling-Based Methods

Evaporative cooling removes heat by accelerating the evaporation of liquid near the skin. Nakajima et al. [16–18] proposed a method using focused ultrasound to enhance water mist evaporation around the skin, providing localized and rapid cooling with spatial precision. However, the system relies on large phased-array ultrasonic transducers and may introduce minor tactile sensations during operation, posing challenges for integration into compact wearable devices. Another notable evaporative approach is the ALCool system by Hamazaki et al. [9]. This system places alcohol-soaked cotton pads near the skin and uses a fan to enhance evaporation. This design is both compact and wearable, offering a noticeable cooling effect. However, a significant limitation is that the system does not control the alcohol concentration, which tends to decrease over time. This leads to an unstable cooling sensation, which compromises the consistency and reliability of the user feedback.

2.6 Positioning of This Study

While numerous cooling feedback methods have been explored, many existing systems are limited by requirements such as direct skin contact, reliance on airflow or bulky components, or unstable sensation delivery. These constraints reduce their suitability for integration into head-mounted or wearable VR devices, particularly in dynamic and event-driven interaction contexts.

This study presents ChillFactor, a non-contact cooling feedback system based on evaporative cooling, which achieves its effect through ultrasonic atomization of an alcohol solution. In contrast to previous systems where feedback became unstable as alcohol concentration decreased, ChillFactor uses a solution with a consistent concentration, enabling a relatively stable cooling sensation near the skin. With its high responsiveness and compact design, ChillFactor is highly suitable for integration into VR headsets, providing cooling feedback synchronized with virtual events to enhance subjective presence and immersion.

3 Physical Evaluation of Non-Contact Alcohol-Based Cooling

To inform the subsequent system design and VR integration, we first conducted a set of physical experiments to characterize the cooling behavior of alcohol mist generated by ultrasonic atomization. We focused on two aspects: (1) the relationship between the atomizer duty cycle and mist output volume, and (2) the impact of mist output and spraying distance on local skin surface temperature. The data informed our parameter selection, including mist output and spray distance, for headset integration.

3.1 Materials and Measurement Setup

3.1.1 Alcohol Solution Preparation

We prepared a 20 % alcohol solution as the cooling medium for ultrasonic atomization. The solution was manually mixed using anhydrous alcohol (≥99.5 %, plant-fermented, Daiyo Pharmaceutical / B005SN0DQU) and purified water of cosmetic grade (Daiyo Pharmaceutical / B00SIIX9JA) in a volumetric ratio of 1:4. All components were selected from commercially available products commonly used in the formulation of facial cosmetics, ensuring suitability for human-facing applications. The alcohol concentration was set to 20 % based on a trade-off between evaporation efficiency and skin safety. While higher alcohol concentrations can promote faster evaporation and reduce liquid residue, they may increase the risk of skin irritation. We therefore adopted a concentration commonly used in cosmetic formulations for direct skin contact in Japan, which typically do not exceed 20 % alcohol. As shown in Fig. 2 (a), the solution was freshly prepared before each experimental session in a single-use quantity, typically 50 mL, and stored in individual brown glass dropper bottles (Ease / B01LXJ6Q1G) to minimize evaporation and light exposure.

3.1.2 Ultrasonic Atomizer Configuration

As shown in Fig. 2 (a), we used an ultrasonic mist generation module (Ren He / B08Z3GXYPK), consisting of a piezoelectric atomizing

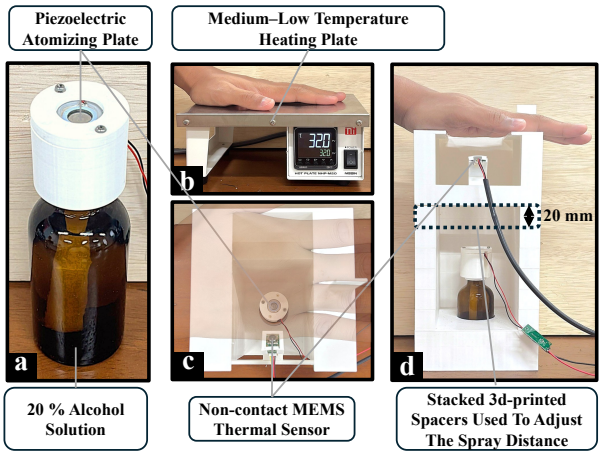


Fig. 2: Experimental setup for physical evaluation of non-contact alcohol-based cooling. (a) A piezoelectric ultrasonic atomizer is used to generate mist from a 20 % alcohol solution. (b) A medium-low temperature heating plate is used to pre-condition the participant's hand to a consistent skin temperature (32 ℃). (c) A non-contact MEMS thermal sensor is positioned at a 45-degree angle to monitor surface temperature without obstructing mist deposition. (d) The entire test structure is built using stacked 3D-printed spacers (20 mm per layer) to manually adjust the spray distance between the atomizer and the skin.

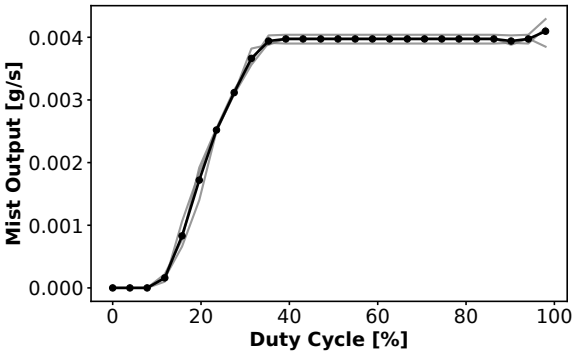


Fig. 3: Mist output under varying duty cycles. Light gray lines represent individual trials, and the black line represents the averaged output across three measurements.

plate and a 5 V USB-powered control board (PCBA), operating at a nominal frequency of 113 kHz. A MOSFET driver module (Youmile / B084VNKLFL) was used to control power delivery to the atomizer. An ESP32 microcontroller, powered via 5 V USB, generated pulse-width modulation (PWM) signals through a GPIO pin to drive the gate input of the MOSFET. The duty cycle of the PWM signal was adjusted to modulate the mist output during operation.

3.1.3 Experimental Environment

All experiments were conducted in an air-conditioned room, with the ambient temperature maintained at 24 to 26 °C and relative humidity ranging approximately from 65 to 70 %, as measured using a digital temperature and humidity meter (ThermoPro / TP-49). No direct airflow was applied to the atomization or measurement area. Temperature and humidity were controlled using a standard air conditioning system.

3.2 Mist Output under Varying Duty Cycles

Mist output was quantified using a digital precision balance (UXILAII / B0CGLTGVTB, 300 g capacity, 0.001 g resolution). The PWM duty cycle was varied from 0 % to 98 % in 4 % increments. For each condition, the solution mass was recorded before and after 100 s of continuous operation, and the output rate (g/s) was calculated accordingly. Each condition was measured three times, and the results were averaged.

Fig. 3 illustrates the measurement results, where the light gray lines represent individual trials and the black line represents the averaged output across three measurements. When the duty cycle was below 10 %, the mist output was negligible. Between 11.8 % and 31.4 %, the output increased rapidly from 0.0002 g/s to 0.0037 g/s, representing a near-linear response region of the atomizer. Beyond 35.3 %, the mist output reached a plateau, maintaining a nearly constant value of approximately 0.0040 g/s despite further increases in duty cycle. These results were used to calibrate the cooling feedback intensity in subsequent experiments.

3.3 Cooling Performance at Different Mist Outputs and Distances

This experiment aimed to preliminarily evaluate the system's physical cooling performance under different mist intensities and spraying distances. As the goal was to measure objective temperature changes rather than subjective sensation, a single participant (the author) was involved.

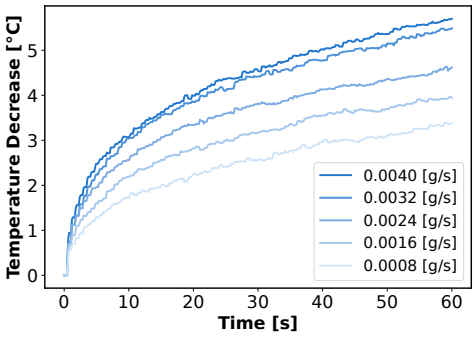
To minimize variability in baseline skin temperature, the participant rested quietly for 10 minutes before the experiment to achieve thermal equilibrium. As shown in Fig. 2 (b), the initial palm temperature was measured as 32 °C. A medium–low temperature heating plate (NHP-M20, NISSIN) was set to the same temperature. Before each trial, the participant placed their palm on the plate for approximately 3 minutes to stabilize skin temperature under consistent conditions.

The spray stimulus was applied continuously for 60 s, and the skin temperature was recorded using a non-contact MEMS thermal sensor (D6T series, OMRON) with a resolution of 0.06 °C and a data update interval of 300 ms. As shown in Fig. 2 (c), the sensor was positioned at a 45-degree angle to the palm to avoid interfering with mist deposition, and aligned to the center of the spraying area. The D6T sensor provides a 4×4 array of temperature readings; to represent the overall skin surface temperature, we computed the average of all 16 pixel values for each frame.

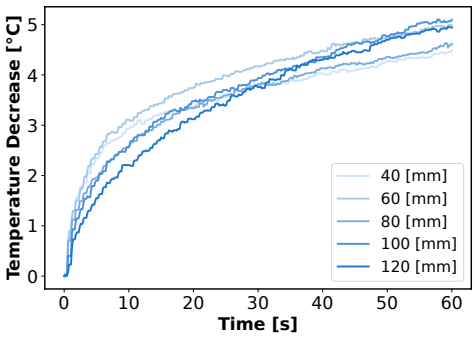
Two sets of conditions were tested. First, at a fixed spray distance of 80 mm, five mist output levels (0.0008, 0.0016, 0.0024, 0.0032, and 0.0040 g/s) were tested. Second, at a constant mist output of 0.0024 g/s, five spray distances (40, 60, 80, 100, and 120 mm) were examined. As shown in Fig. 2 (d), the spray height was manually adjusted using stacked 3D-printed spacers, each 20 mm thick. Each condition was repeated three times and the mean temperature response was used for the analysis.

As shown in Fig. 4 (a), the temperature decrease intensified over time under all mist output conditions, with higher mist levels resulting in more pronounced cooling effects. Greater mist output implies a larger amount of liquid available for evaporation per unit time, thereby increasing the amount of heat absorbed from the skin. This effect was evident within the first few seconds after the onset of spraying, indicating that the system exhibits a high degree of temporal responsiveness. Specifically, within the first 5 seconds of spraying, a clear drop in skin temperature was observed across all conditions: approximately 1.6°C under the lowest mist output (0.0008 g/s) and up to around 2.6°C under the highest output (0.0040 g/s), yielding a difference of over 1°C. It should be noted that the temperature changes observed during the initial 1 to 2 seconds may have been influenced by interference from the mist itself, resulting in some measurement fluctuations. Therefore, we primarily use the temperature decrease at 5 seconds as an indicator to evaluate the cooling performance of the system. These results suggest that even within a short duration, the mist output level has a substantial impact on the cooling performance. These findings indicate that adjusting the mist output can effectively modulate the intensity of cold perception within a certain range, offering a practical parameter for altering feedback strength and supporting adaptation to diverse interactive scenarios.

As shown in Fig. 4 (b), no clear monotonic relationship was observed between spray distance and overall temperature decrease. During the first 45 s, the 60 mm condition produced the greatest cooling effect,



(a)



(b)

Fig. 4: Temperature changes under different mist output (a) and spray distance (b) conditions.

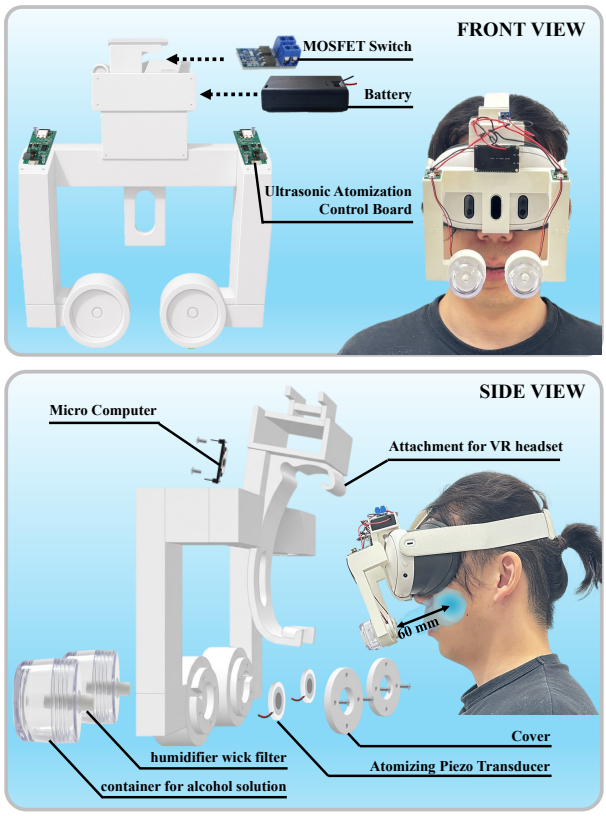


Fig. 5: Hardware configuration.

while beyond 45 s, the 100 mm condition gradually exceeded it in temperature reduction. These trends may result from differences in mist dispersion patterns and the effective skin coverage area at different distances. At the shortest distance of 40mm, visible liquid residue was observed on the skin, which could affect both comfort and the consistency of the thermal sensation.

These results provide valuable insights for the subsequent system design. In VR applications, where cold stimuli are often triggered and switched rapidly in response to user interactions, the initial rate of cooling is particularly important. Based on these observations, a spray distance of 60 mm was selected for the subsequent system implementation. By adjusting the mist output, changes in skin temperature can be induced, which may allow for the presentation of cold sensations with varying intensities.

4 Hardware Design and Integration

This section describes the hardware design and integration of the proposed cooling feedback interface, which delivers non-contact cooling via alcohol mist evaporation for use in VR headsets.

As shown in Fig. 5, the mist was directed toward the user's cheeks, selected as the target stimulation area. Although regions near the philtrum exhibit higher thermal sensitivity, they were intentionally avoided to prevent mist from entering the mouth or nasal cavity. Based on the results of the preceding experiments, the spray distance was set to 60 mm. This value was determined using the facial geometry of the designer.

The system hardware consists of a central control module and two symmetric mist generation units. The control module is equipped with a microcontroller (ELEGOO / ESP-WROOM-32), which handles wireless communication and synchronized control of mist output. PWM signals generated by the microcontroller are used to drive a MOSFET switch (Youmile / B084VNKLFL), regulating current flow to a shared ultrasonic atomization control board. This configuration enables fine control over the output power delivered to the piezoelectric transducers in both mist units. Power is supplied by a battery pack (Kaito Denshi / B089PXW545) containing three AAA cells, providing a total of 4.5 V.

Each mist generation unit comprises four key components: a liquid container holding a 20 % alcohol solution, a wick that continuously delivers liquid to the transducer surface, a piezoelectric atomizer that converts liquid into fine mist, and a cover structure that mechanically secures the atomization unit in place. The atomizer and its control components are consistent with those described in Section 3. The alcohol container is refillable, allowing users to replenish the solution during extended use.

All components are mounted on a supporting bracket designed for attachment to the front of a VR headset, ensuring precise alignment of the mist with the target area. The bracket was fabricated using a 3D printer (Bambu Lab / X2 Carbon) with white ABS filament (Bambu Lab / ABS White). The total weight of the device is 208 g without liquid and 240 g when fully filled. At the maximum mist output rate of approximately 0.0040 g/s, the system can operate continuously for about one hour, which is sufficient for most VR usage scenarios.

5 User Study

In this section, we conducted two user studies to evaluate the effectiveness of the proposed cooling feedback system. The first experiment aimed to assess the perceived intensity and temporal responsiveness of the cooling sensation generated by the system in a controlled setting. The second experiment involved immersive VR scenarios, designed to investigate whether the system could enhance users' perception of cold sensations during interactive experiences.

5.1 Participants

A total of 12 paid participants (mean age = 25.9 years, SD = 2.6; age range: 23–30 years; 6 females and 6 males) took part in the study. All participants completed both experiments. None of them were involved in the development of the system. Participants received compensation equivalent to approximately 8 USD for their time. The participant

recruitment and experimental procedures were approved by the Life Science Research Ethics and Safety Committee at The University of Tokyo (Protocol No. 24-523, approved on February 14, 2025), and conducted in accordance with the institution's ethical guidelines. All participants provided written informed consent before participation.

5.2 Experimental Environment

All experiments were conducted in a soundproof room to ensure a consistent sensory environment and minimize external auditory distractions. The ambient temperature and humidity were controlled using a standard air conditioning system. The temperature was maintained at approximately 24 to 26 °C, and the relative humidity was kept within the range of 65 to 70 %, as measured using a digital temperature and humidity meter (ThermoPro / TP-49). The room was free of direct airflow and sunlight and stable indoor lighting was used throughout. In both experiments, participants wore the cooling feedback device developed in this study, which was attached to a Meta Quest 3 headset using a custom 3D-printed bracket. The mist outlet was designed to be approximately 60 mm from the user's cheek, based on the facial geometry of the designer. Subsequently, this design target was validated to fall within a practical range of approximately 55 to 65 mm in other participants, accommodating individual differences in facial structure.

5.3 Evaluation of Cold Perception Characteristics

To evaluate the perceptual characteristics of the proposed system in a controlled setting, we examined the onset and offset latency of the perceived cooling sensation, as well as its intensity, under different mist output conditions. The objective was to determine whether the system can deliver clearly perceivable and responsive cooling feedback suitable for interactive applications.

5.3.1 Experimental Procedures

Five mist output levels (0.0008, 0.0016, 0.0024, 0.0032, and 0.0040 g/s) were selected as experimental conditions. Each condition was repeated three times in a randomized order, resulting in a total of 15 formal trials per participant. Prior to the formal trials, two practice trials were conducted to familiarize participants with the procedure.

As shown in Fig. 6, at the beginning of the experiment, participants were seated and equipped with a VR headset featuring a cooling feedback interface, as well as noise-canceling headphones (JBL / Tour Pro 2). In each trial, a 5-second idle period was first given, followed by 5 seconds of continuous cold stimulation, and then another 5 seconds with the stimulation turned off. Participants were instructed to press and hold a button on the VR controller when they first perceived the cold sensation, and to release the button when they no longer perceived it. The timing of their button presses and releases was recorded in real time to calculate the perceptual onset latency t_{po} (the time from stimulus onset to initial perception) and perceptual offset latency t_{pf} (the time from stimulus offset to the end of perception). To minimize potential distraction or bias from visual cues, only the current trial number was displayed in the virtual environment.

At the end of each trial, participants were presented with a 7-point Likert scale and instructed to use the VR controller to select the option that best reflected the intensity of the cooling sensation they experienced. The scale ranged from 1 (representing "No cooling sensation") to 7 (representing "Extremely strong"), with 4 indicating a "Moderate" cooling sensation. Participants were required to select the rating that best corresponded to the intensity of the sensation they had just experienced.

Additionally, a 30-second rest period was implemented after each trial. The authors verified that this duration was sufficient for the participants' skin temperature to naturally return to its initial state. During this time, participants were allowed to remove the headset and move freely.

Upon completion of all trials, participants provided qualitative feedback through an open-ended interview, describing the perceived range of cooling sensations using free-form responses (e.g., "as cold as an ice cube" or "like a cool breeze").

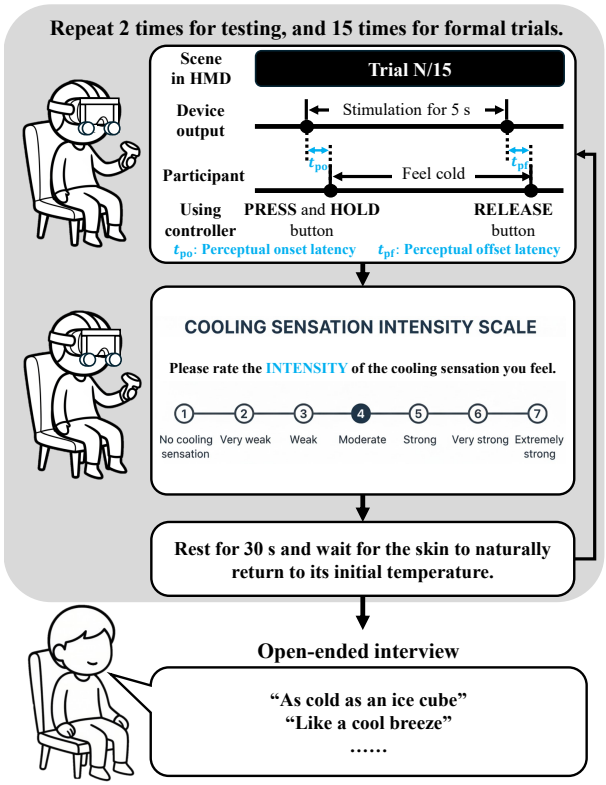


Fig. 6: Experimental procedures for evaluating cold perception, including stimulation, response latency measurement, intensity rating, and qualitative feedback.

5.3.2 Results

Fig. 7 shows the perceptual response time data for each mist output level. The shaded gray region denotes the stimulation period (5–10 s). Colored lines represent participant-level binary response trajectories, and the bold black line indicates the overall binary average response. This rounding enabled consistent extraction of onset (t_{po}) and offset (t_{pf}) latencies from the average trajectory.

At the lowest mist level (0.0008 g/s), only one participant recorded cold sensation, with most participants reporting no perception. As a result, the average response remained at zero and latency metrics were not calculated. For mid-range outputs (0.0016–0.0032 g/s), both t_{po} and t_{pf} clustered around 1000 ms. At the highest mist level (0.0040 g/s), both latency measures were reduced, with t_{po} averaging approximately 661 ms and t_{pf} approximately 851 ms. This demonstrates that higher output enabled faster and more consistent perception of cooling. Notably, the onset latency approaches values reported in foundational psychophysical studies — for instance, Frühstorfer et al. [8] found average cold detection times around 529 ms. Achieving such responsiveness using a non-contact, miniature system validates its suitability for interactive cooling feedback applications.

To examine the impact of mist output on perceived coldness intensity, we conducted a Kruskal-Wallis test. The analysis revealed a significant main effect, $\chi^2 4 = 113.39$, $p = 1.377 \times 10^{-23}$, indicating that at least one mist level produced a significantly different intensity rating. We then conducted pairwise Wilcoxon rank-sum tests between adjacent mist levels to assess whether perceived intensity increased progressively. As shown in Fig. 8, significant differences were found between 0.0008 and 0.0016 g/s ($p < .001$) and between 0.0032 and 0.0040 g/s ($p < .001$), while intermediate comparisons (0.0016–0.0032 g/s) were not significant ($p > 0.05$).

These results indicate a clear upward trend in coldness perception across mist levels. Particularly, perceptual intensity increased significantly in the transitions from 0.0008 to 0.0016 g/s and from 0.0032 to 0.0040 g/s, while remaining statistically unchanged between the

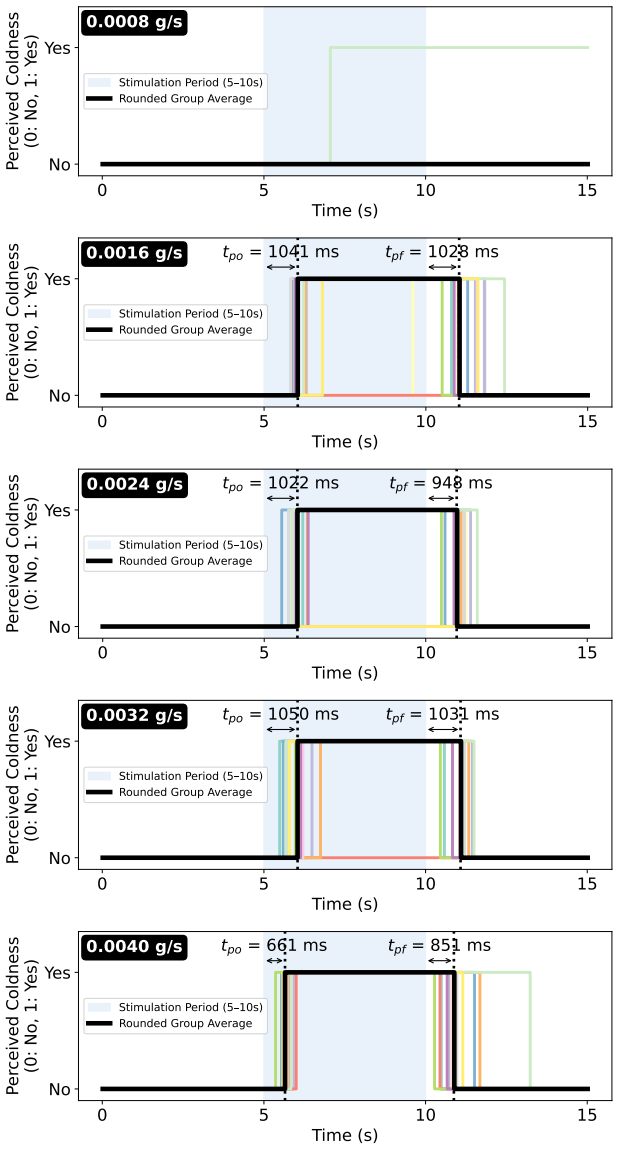


Fig. 7: Perceptual onset and offset latencies across mist output levels (t_{po}: perceptual onset latency, t_{pf}: perceptual offset latency). Colored lines show the responses of individual participants, while the black line represents the overall binary average across all trials.

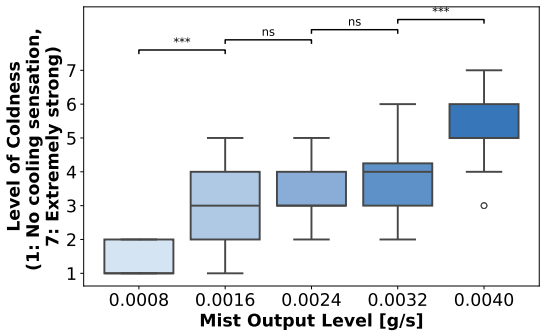


Fig. 8: Perceived coldness intensity across mist output levels (g/s) (***: $p < 0.001$; ns: $p > 0.05$).

Table 1: Summary of key performance parameters of ChillFactor.

Parameter	Value / Specification
Mist Output Rate	0.0008–0.0040 g/s
Effective Spray Distance	60 mm
Perceptual Onset Latency (t_{po})	661 ms (at 0.0040 g/s)
Typical Temperature Drop	2.6 °C within 5 s

mid-range levels. This suggests that the system is capable of producing at least three distinct levels of cold perception through mist output modulation. The key performance parameters derived from these quantitative evaluations, combined with system specifications, are summarized in Table 1.

Following the quantitative evaluations, participants offered qualitative descriptions of their cold sensations. Stronger impressions were described with terms such as "cold air from an air conditioner," "walking in the winter," or "snowy weather," whereas weaker sensations were described as "a breeze," "opening a refrigerator," or "autumn air." These varied subjective expressions underscore the system's ability to evoke a recognizable and gradable spectrum of cold impressions under different output conditions.

5.4 Assessment of Cooling Feedback in VR Scenarios

To assess the applicability of cooling feedback in immersive environments, we conducted a user study in VR to examine whether cold intensity and real-time responsiveness enhance presence and realism.

As shown in Fig. 9, we present a story-driven VR gift-delivery experience set on a snowy night, in which participants role-play a Santa-like courier delivering six gifts to six distinct homes. The environment alternates between a cold outdoor snowfield and indoor spaces with no thermal feedback, producing frequent, context-appropriate state changes at door thresholds. The scene comprises an outdoor hub and six spatially distributed houses so that each delivery involves a brief outdoor segment rather than repeated actions at a single doorway. The task does not implement navigation aids or pathfinding; participants rely on labels above gifts and houses to perform one-to-one matching, approach the corresponding door, step indoors to confirm delivery, and return outside to proceed to the next house. Consequently, each condition yields twelve transitions (outdoor→indoor and indoor→outdoor per gift). Thermal output switches immediately based on context: cooling is enabled outdoors and disabled upon entry to interiors. Aside from cold intensity, visuals, audio, locomotion, and interactions are identical across conditions. The layout targets approximately 4–6 minutes of play per condition, and the spatial arrangement naturally encourages repeated shuttling between outdoor and indoor segments.

5.4.1 Experimental Procedures

Before the formal study, participants completed a 1–2 minute familiarization in the Unity6 default VR template scene (no thermal feedback, not analyzed) to practice smooth locomotion with orientation adjustments and basic object manipulation (near grab; ray-based grab if needed). The study employed a within-subjects, single-factor, three-level design with cold intensity (No, Low, High) as the factor. To mitigate learning and fatigue effects, we used a fully counter-balanced design: the six permutations of A, B, C, where A = No, B = Low, and C = High, were assigned with equal frequency across participants. Two participants were assigned to each sequence, thereby balancing starting-position frequencies and first-order carryover effects. Low intensity used 0.0016 g/s and High intensity used the system's maximum output of 0.0040 g/s; the No condition duplicated visuals, audio, locomotion, and interactions but suppressed thermal output. In each condition, participants started at the outdoor hub and completed six deliveries as described in Section 5.4; the condition ended once all gifts were delivered.

Immediately after each condition, participants completed the questionnaire shown in Table 2. Items Q1, Q2, Q4, and Q5 were adapted from the Igroup Presence Questionnaire (IPQ) [23], covering the dimensions of involvement, general presence, and spatial presence. Item

Table 2: Subjective questionnaire used in the study. Items Q1, Q2, Q4, and Q5 are adapted from the Igroup Presence Questionnaire (IPQ); Q3, Q6, and Q7 address satisfaction and thermal-specific perceptions. All items use a 7-point Likert scale (1 = Strongly Disagree, 4 = Neutral, 7 = Strongly Agree).

ID	Question Item	Target Dimension (for Analysis)
Q1	My attention was fully focused while I was in the virtual environment.	Involvement
Q2	I had a strong feeling of "being there" in the virtual world.	General Presence
Q3	Overall, I was satisfied with this experience.	Experience Satisfaction
Q4	I felt surrounded by the virtual world.	Spatial Presence
Q5	I was aware of the real-world surroundings (e.g., room temperature, ambient sounds).	Spatial Presence (Reverse)
Q6	I could clearly perceive temperature changes when moving between outdoors and indoors.	Thermal Salience
Q7	The cold sensation felt appropriate and believable for the snowy outdoor scenes.	Thermal Fidelity

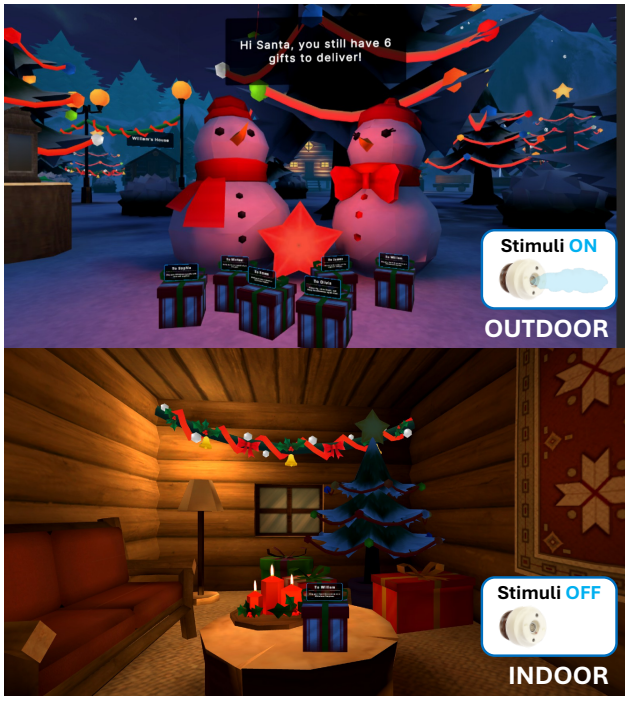


Fig. 9: Story-driven VR scenario for the gift-delivery task. Participants alternated between outdoor snowy environments, where cooling feedback was enabled (Stimuli ON), and indoor spaces, where feedback was disabled (Stimuli OFF), creating repeated thermal transitions aligned with the virtual context.

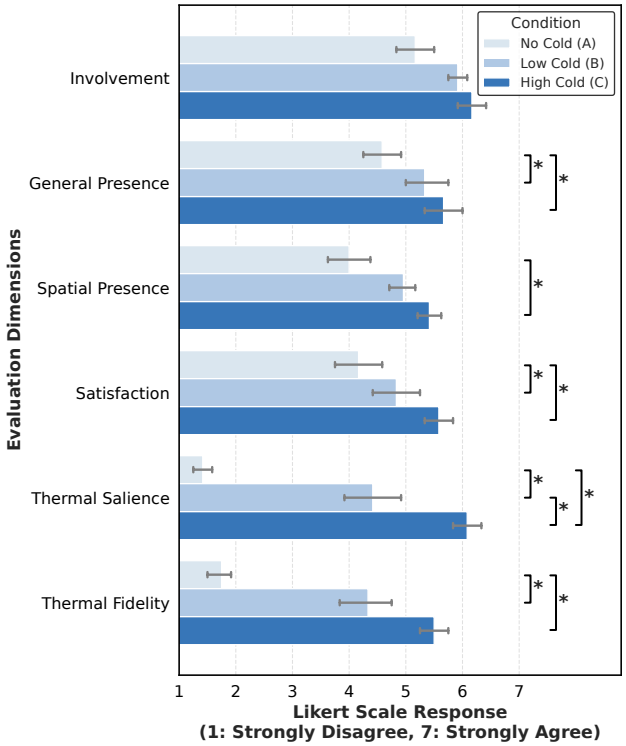


Fig. 10: Subjective evaluation results across three cooling intensities. Error bars represent standard error. Items are aggregated following the IPQ framework: Involvement (Q1), General Presence (Q2), and Spatial Presence (Q4 and reverse-coded Q5). Significance markers (*: adjusted $p < .05$) denote Bonferroni-corrected post-hoc comparisons. Large effect sizes ($W \geq 0.37$) were observed for all presence-related dimensions.

Q3 was included to assess overall experience satisfaction, while Q6–Q7 were thermal-specific items evaluating the salience of temperature changes during outdoor–indoor transitions and the perceived fidelity of the cold sensation. After completing all three conditions, we conducted a 3–5 min semi-structured interview focusing on transition perception, believability, and intensity preferences. Example prompts included (i) perceptions of outdoor–indoor temperature changes; (ii) moments when the cooling feedback felt believable or not and why; and (iii) comparisons and preferences among No/Low/High intensities.

5.4.2 Results

Fig. 10 summarizes participants' subjective ratings across the three cooling feedback conditions: "No Cold," "Low Cold," and "High Cold." Ratings were given on a 7-point Likert scale (1 = Strongly Disagree, 7 = Strongly Agree), with standard error (SE) shown as error bars. Following the Igroup Presence Questionnaire (IPQ) framework, we aggregated items into focused dimensions: Involvement (Q1), General Presence (Q2), and Spatial Presence (mean of Q4 and reverse-coded Q5). We assessed data distribution via Shapiro-Wilk tests; as normality was violated for several dimensions, we employed Friedman tests for main effects and Bonferroni-corrected Wilcoxon signed-rank tests for post-hoc comparisons (except for General Presence, where RM-ANOVA was used).

Analysis revealed significant main effects of cooling intensity across all presence-related dimensions, including General Presence ($F\left(2,22\right) = 12.29, p < .001, \eta_p^2 = 0.53$), Spatial Presence ($\chi^2\left(2\right) = 12.05, p = 0.002, W = 0.50$), and Involvement ($\chi^2\left(2\right) = 8.82, p = 0.012, W = 0.37$). Post-hoc tests confirmed that the High Cold condition significantly outperformed the No Cold condition in General Presence and Spatial Presence (adjusted $p < .05$). For Involvement, although no pairwise significance was reached after Bonferroni correction, a strong positive trend was observed in favor of High Cold. These results suggest that high-intensity cooling feedback enhances perceived presence and involvement in VR, supported by moderate to large effect sizes (Cramér's $W = 0.37$–0.50).

For the thermal-specific items, the High Cold condition was rated significantly higher than both No Cold and Low Cold in terms of per-

ceived thermal salience (Q6) and thermal fidelity (Q7) ($\chi^2(2) \geq 20.42$, adjusted $p < .001$), indicating stronger alignment between thermal sensation and environmental cues. While Low Cold also outperformed No Cold on these items (adjusted $p < .001$), High Cold maintained a notable advantage over Low Cold (adjusted $p = 0.023$ for Q6), highlighting the impact of intensity. Overall satisfaction (Q3) similarly showed a significant subjective preference for High Cold over No Cold ($\chi^2(2) = 16.19$, adjusted $p = 0.006$).

Semi-structured interviews further contextualized these findings. Most participants reported perceivable temperature changes during indoor–outdoor transitions, especially under the High Cold condition. Some noted that when the mist entered their nose—though unintended—it evoked the familiar feeling of stepping into winter air, enhancing naturalness through localized and directional cooling. Several participants commented that facial-only cooling reduced overall believability, particularly when the rest of the body remained warm. Others found that alignment with visual and auditory cues (e.g., blowing wind, rustling trees) strengthened the illusion. Some also suggested that constant cooling during locomotion detracted from realism and recommended dynamic feedback tied to movement, such as stronger cooling during fast motion and softer output when stationary. In terms of preference, the majority favored the High Cold condition, describing it as the most realistic and engaging. However, some participants noted that in scenes lacking clear visual cues of coldness, High Cold felt overly intense, whereas Low Cold provided a more balanced experience between intensity and plausibility. A few participants also noted that seasonality could affect thermal perception. Cooling feedback might feel more natural in summer, while in winter, it could highlight mismatches if indoor warmth is not adequately simulated.

Overall, participants agreed that cooling feedback, particularly when timely, sufficiently intense, and contextually synchronized, can meaningfully enhance realism and presence in VR. Nonetheless, balancing intensity with comfort remains important. Future systems may benefit from adaptive thermal control responsive to context and user movement.

6 Discussion

This study systematically examined the feasibility and potential of non-contact cooling feedback based on alcohol mist evaporation in VR through a combination of physical evaluation and user-centered experiments.

In the initial physical experiments, we confirmed that the alcohol-based mist cooling mechanism exhibited clear temporal responsiveness and controllable output. Skin temperature dropped noticeably within a few seconds under various mist intensities, with a 60 mm spray distance yielding the most stable performance. These results provided quantitative design parameters for system integration and demonstrated the mechanism's suitability for brief, event-driven interactions in VR.

In the controlled perceptual study, the system demonstrated reliable detectability and gradability of cold sensations. Notably, under high mist output, the average perception onset latency was approximately 660 ms, approaching psychophysical benchmarks for traditional cold stimuli. Participants were also able to clearly distinguish between different intensity levels, suggesting that mist output modulation effectively encodes perceptual coldness. Qualitative feedback revealed that users associated each intensity with distinct real-world experiences, such as "air conditioning" or "stepping outside in winter," indicating that the system not only induces physical cooling but also evokes vivid perceptual representations.

In the immersive VR task, cooling feedback significantly enhanced users' subjective ratings of presence and engagement. The high-intensity condition led to substantial improvements in perceived attentional focus, spatial immersion, and overall satisfaction. Participants also rated thermal transitions and contextual appropriateness more positively when cooling feedback was enabled, aligning with the principle of crossmodal congruency [25]. Interview data highlighted that synchronization between cold sensations and environmental cues (e.g., snow visuals, wind sounds) contributed to the perceived thermal realism reported by users. Although mist entering the nose was not part of the design, some users reported that it enhanced the illusion of cold outdoor air, showcasing the system's potential in multisensory integration. Further studies are needed to investigate the role of such unintended but synergistic effects in immersive interaction design.

7 Limitations and Future Work

Despite promising results, several limitations were identified that suggest directions for future improvement.

The physical evaluation in this study was conducted on a single participant and therefore does not capture inter-individual differences in cooling and evaporation behavior. Factors such as skin thickness, moisture, and surface conditions may affect heat transfer and evaporation rates, potentially leading to variability across users. While our goal was to assess the physical feasibility and temporal characteristics of the proposed cold feedback mechanism rather than to model individual physiological differences, we acknowledge that the reported measurements may be individual-dependent. Future work will include evaluations with a larger number of participants as well as reference measurements on non-living surfaces to better isolate system-level behavior from human variability.

This work does not include an explicit theoretical modeling or quantitative validation of the evaporative heat transfer process. While the proposed cooling mechanism is based on the well-known principle of latent heat absorption during evaporation, our goal was to empirically evaluate the feasibility and temporal characteristics of the alcohol mist–based cooling interface rather than to develop or validate a detailed thermodynamic model. Future work will include simple analytical modeling as well as controlled reference measurements on non-biological surfaces to more directly relate the observed cooling behavior to theoretical expectations.

This study focuses on the onset and short-term offset characteristics of cooling under brief stimulation and does not examine temperature recovery behavior following prolonged or repeated cooling cues. In the response time measurement experiment, the cooling stimulus duration was limited to 5 s, and temperature recovery was observed only under this condition through passive heat exchange between the skin and the environment. As a result, recovery dynamics after longer stimulation periods or repeated cooling events were not quantitatively characterized. Future work will include systematic measurements of temperature recovery under extended and repeated stimulation to better understand sensation persistence, comfort, and potential cumulative effects.

In the VR task, cooling events occurred relatively frequently as part of the interaction flow. Because temperature recovery between consecutive events was not explicitly controlled or enforced, residual cooling effects may have accumulated across trials. This could lead to adaptation effects that reduce perceived cooling intensity, particularly for mid-level stimulation conditions, and may partially explain the lack of significant differences observed in some cases. Future work should consider spacing out cooling events, enforcing baseline temperature recovery between stimuli, or explicitly modeling adaptation effects to better isolate perceptual responses.

The system uses a 20% low-concentration alcohol solution, selected based on a trade-off between evaporation efficiency and skin safety, consistent with established cosmetic aerosol standards [24]. However, its long-term or frequent use near sensitive facial regions, such as the nasal cavity, remains insufficiently assessed. Future work should further optimize material selection and liquid handling, systematically examine different alcohol concentrations and their safety-performance trade-offs, or improve the physical design to avoid mist entry into the nose, thereby enhancing safety and hygiene in practical deployment. In addition, because the mist is released in close proximity to the face, potential risks to the eyes and respiratory system have not been systematically evaluated in this study. Future designs should incorporate precautionary measures such as directional flow control, physical shielding, or spatial offsets to minimize unintended exposure to the eyes and inhalation pathways. Furthermore, we acknowledge that this study did not include quantitative validation of alcohol concentration levels or inhalation exposure limits. Future work will prioritize quantitative safety evaluations, including dermatological testing, inhalation exposure assessment, and user comfort validation, to enhance the technical rigor

and safety evaluation of the system.

Currently, the system delivers cooling feedback only to the cheek region. While effective, this localized stimulation may create perceptual mismatches with other body areas, which could diminish overall ecological realism and immersion. Several participants noted that the limited spatial feedback reduced realism. Future implementations may benefit from extending cold stimuli to additional regions such as the neck, arms, or upper torso, enabling greater thermal coherence and supporting more complex spatial temperature illusions.

All experiments were conducted under relatively high ambient humidity (65–70%), which may slow evaporation and affect perceived cooling intensity. The influence of varying humidity conditions was not examined and is left for future work. While mist output is modulated via PWM, the spatial behavior of the alcohol mist—such as droplet size, dispersion profile, and evaporation under varying ambient conditions—has not yet been quantitatively characterized. Future research could employ high-speed imaging, particle tracking, or computational fluid dynamics simulations to analyze mist dynamics and improve the consistency of thermal delivery.

The current user study involved 12 participants aged 23–30, with a balanced gender distribution. While sufficient for preliminary validation, the sample lacks broader diversity in terms of age range, nationality, and thermal adaptation backgrounds, which may limit the generalizability of the reported findings. Future studies should include participants from a wider range of demographic and cultural backgrounds, and consider seasonal comparisons (e.g., winter vs. summer) to better understand cross-context variability in cold sensation perception.

Furthermore, the current evaluation of presence and engagement relies primarily on standardized subjective questionnaires. While the aggregated IPQ scales provide a validated measure of user experience, they do not capture the physiological or behavioral dimensions of immersion. We acknowledge that incorporating objective measures, such as heart-rate variability (HRV), skin conductance, or behavioral indicators like gaze concentration and task performance, would provide a more holistic and robust validation of the claimed increase in immersion. Future work will aim to include these multimodal evaluation metrics to complement self-report data and further clarify the physiological impact of reactive cooling feedback.

From a conceptual perspective, this work does not explicitly model the cognitive or affective mechanisms underlying thermal immersion and multisensory integration. While the results demonstrate perceptual and psychological benefits of cooling feedback, the interaction between thermal cues and other sensory modalities (e.g., visual and auditory inputs) is interpreted at an empirical level rather than within a unified theoretical framework. Future work could draw on established models of multisensory congruence and affective processing to better explain how and why localized cooling enhances presence, as well as to clarify the limits of such effects.

In addition, although this work focuses on alcohol mist–based evaporative cooling, a systematic conceptual comparison with other non-contact cooling approaches (e.g., airflow-based or ultrasonic phased-array systems) is beyond the scope of the current study. Future research could further contextualize ChillFactor's design choices by comparing responsiveness, comfort, and portability across different non-contact cooling paradigms.

Overall, ChillFactor presents a compact, responsive, and non-contact cooling feedback solution for immersive systems. Future work will explore dynamic feedback modulation based on user motion, spatial thermal distribution, and multi-sensory integration to further enhance realism and personalization in VR interaction.

8 Conclusion

This paper presented ChillFactor, a lightweight, non-contact cooling feedback system for VR headsets. By employing evaporative cooling from an ultrasonically atomized alcohol solution, the system avoided airflow artifacts and achieved a compact, responsive design with adjustable output levels. Utilizing this mechanism, the system produced rapid cooling, reducing skin temperature by approximately 2.6 °C within 5 s, which was sufficient to induce an almost immediate cold sensation. Perceptual testing further showed that the average onset latency for cold sensation under high-output conditions was 661 ms, indicating adequate responsiveness for interactive applications. In VR evaluations, the system was found to significantly enhance general presence, spatial presence, and overall satisfaction. Furthermore, although involvement only showed a strong positive trend in statistical analysis, high-intensity cooling feedback consistently received the highest ratings for both salience and thermal realism, demonstrating its superior perceptual performance. These findings suggest the feasibility of ultrasonic evaporative cooling as a non-contact thermal feedback method in VR and indicate its potential to enhance perceived multisensory experiences. Furthermore, our measurements of key parameters provide valuable references for haptic interaction design.

Acknowledgments

This work is supported in part by Suntory Holdings Limited, JSPS KAKENHI JP24K23883, JP24K02969 and JP24K22316. The authors acknowledge the use of ChatGPT (developed by OpenAI) for English proofreading and language refinement throughout this manuscript. No content was generated solely by the AI system; the authors were responsible for all technical content, analysis, and interpretation. The AI-assisted edits were limited to improving grammar, clarity, and fluency in all sections of the paper.

References

[1] F. Barbosa Escobar, C. Velasco, K. Motoki, D. V. Byrne, and Q. J. Wang. The temperature of emotions. *PloS one*, 16(6):e0252408, 2021. 1

[2] J. Brooks, S. Nagels, and P. Lopes. Trigeminal-based temperature illusions. In *Proceedings of the 2020 CHI conference on human factors in computing systems*, pp. 1–12, 2020. 1, 2

[3] S. Cai, P. Pei, T. Narumi, and K. Zhu. ThermAirGlove: A Pneumatic Glove for Thermal Perception and Material Identification in Virtual Reality. In *Proceedings of the IEEE Conference on Virtual Reality and 3D User Interfaces (IEEE VR 2020)*, pp. 248–257. IEEE, 2020. doi: 10.1109/VR46266.2020.00045 1, 2

[4] S. Cardin, D. Thalmann, and F. Vexo. Head mounted wind. *in Proceeding of the 20th annual conference on Computer Animation and Social Agents (CASA2007)*, pp. 101–108, 2007. 1, 2

[5] J. Citerin, A. Pocheville, and A. Kheddar. A touch rendering device in a virtual environment with kinesthetic and thermal feedback. *in Proceeding of IEEE International Conference on Robotics and Automation*, pp. 3923–3928, 2006. 1, 2

[6] B. Deml, A. Mihalyi, and G. Hanning. Development and experimental evaluation of a thermal display. *in Proceeding of EuroHaptics Conference*, pp. 257–262, 2006. 1, 2

[7] J. Dionisio, V. Henrich, U. Jakob, A. Rettig, and R. Ziegler. The virtual touch: haptic interfaces in virtual environments. *Computer and Graphics*, 21(4):459–468, 1997. 1, 2

[8] H. Fruhstorfer, H. Guth, and U. Pfaff. Thermal reaction time as a function of stimulation site. *Pflügers Archiv*, 335:R49, 1972. 5

[9] T. Hamazaki, T. Takami, K. Ushiyama, I. Mizoguchi, and H. Kajimoto. Alcool: Utilizing alcohol's evaporative cooling for ubiquitous cold sensation feedback. In *Proceedings of the CHI Conference on Human Factors in Computing Systems*, pp. 1–14, 2024. 1, 2

[10] K. Hayakawa, K. Imai, R. Honaga, and M. Sakaguchi. High-speed thermal display system that synchronized with the image using water flow. *in Collection of Haptic Interaction*, pp. 69–74, 2015. 1, 2

[11] H. Ho and L. A. Jones. Material identification using real and simulated thermal cues. *in Proceeding of The 26th Annual International Conference of the IEEE Engineering in Medicine and Biology Society*, 1:2462–2465, 2004. 1, 2

[12] L. A. Jones and H. Ho. Warm or cool, large or small? the challenge of thermal displays. *IEEE Transactions on Haptics*, 1(1):53–70, 2008. 1

[13] Y. Kume, T. Mizuno, and R. Yonezawa. A non-contact thermal display system by higher and lower temperature radiation sources (in japanese). *in Proceeding of The 27th Annual Conference of the Virtual Reality Society of Japan*, p. 4 pages, 2022. 1, 2

[14] Y. Kume and T. Tanaka. A non-contact thermal display with quick response by use of air-flow (in japanese). *in Proceeding of The 24th Annual Conference of the Virtual Reality Society of Japan*, p. 2 pages, 2019. 1, 2

[15] K. Kushiyama, M. Inose, R. Yokomatsu, K. Fujita, T. Kitazawa, M. Tamura, and S. Sasada. Thermoesthesia: about collaboration of an artist and a scientist. *in Collection of ACM SIGGRAPH 2006 Sketches*, p. 2 pages, 2006. 1, 2

[16] M. Nakajima, K. Hasegawa, Y. Makino, and H. Shinoda. Remotely displaying cooling sensation using ultrasound mist beam. *in Proceeding of International AsiaHaptics conference*, pp. 85–87, 2018. 1, 2

[17] M. Nakajima, K. Hasegawa, Y. Makino, and H. Shinoda. Spatiotemporal pinpoint cooling sensation produced by ultrasound-driven mist vaporization on skin. *IEEE Transactions on Haptics*, 14(4):874–884, 2021. 1, 2

[18] M. Nakajima, Y. Makino, and H. Shinoda. Remote cooling sensation presentation controlling mist in midair. *in Proceeding of 2020 IEEE/SICE International Symposium on System Integration (SII)*, pp. 1238–1241, 2020. 1, 2

[19] K. Ogasahara and M. Sakaguchi. Influence on human body by thermal sensation stimulation using wind (in japanese). *in Proceeding of The 24th Annual Conference of the Virtual Reality Society of Japan*, p. 3 pages, 2019. 1, 2

[20] R. L. Peiris, W. Peng, Z. Chen, L. Chan, and K. Minamizawa. Thermovr: exploring integrated thermal haptic feedback with head mounted displays. *in Proceeding of the 2017 CHI Conference on Human Factors in Computing Systems*, pp. 5452–5456, 2017. 1, 2

[21] M. Sakaguchi, K. Imai, and K. Hayakawa. Development of high-speed thermal display using water flow. *in Proceeding of International Conference on Human Interface and the Management of Information*, pp. 233–240, 2014. 1, 2

[22] K. Sato and T. Maeno. Presentation of rapid temperature change using spatially divided hot and cold stimuli. *Journal of Robotics and Mechatronics*, 25(3):497–505, 2013. 1, 2

[23] T. Schubert. The sense of presence in virtual environments: A three-component scale measuring spatial presence, involvement, and realness. *Zeitschrift für Medienpsychologie*, 15:69–71, 04 2003. doi: 10.1026//1617-6383.15.2.69 6

[24] Scientific Committee on Consumer Safety (SCCS). The sccs notes of guidance for the testing of cosmetic ingredients and their safety evaluation, 12th revision. Technical Report SCCS/1647/22, European Commission, 2023. 8

[25] C. Spence. Crossmodal correspondences: A tutorial review. *Attention, Perception, & Psychophysics*, 73(4):971–995, 2011. 1, 8

[26] J. Xu, S. Hasegawa, K. Kiyokawa, N. Ienaga, and Y. Kuroda. Integration of independent heat transfer mechanisms for non-contact cold sensation presentation with low residual heat. *IEEE Transactions on Haptics*, 16(4):770–784, 2023. doi: 10.1109/TOH.2023.3324754 1, 2

[27] J. Xu, Y. Kuroda, S. Yoshimoto, and O. Oshiro. Non-contact cold thermal display by controlling low-temperature air flow generated with vortex tube. In *2019 IEEE World Haptics Conference (WHC)*, pp. 133–138, 2019. doi: 10.1109/WHC.2019.8816089 1, 2

[28] J. Xu, S. Yoshimoto, N. Ienaga, and Y. Kuroda. Intensity-adjustable non-contact cold sensation presentation based on the vortex effect. *IEEE Transactions on Haptics*, 15(3):592–602, 2022. doi: 10.1109/TOH.2022.3187759 1, 2

[29] A. Yamamoto, B. Cros, H. Hasgimoto, and T. Higuchi. Control of thermal tactile display based on prediction of contact temperature. *in Proceeding of IEEE International Conference on Robotics and Automation*, 2:1536–1541, 2004. 1, 2